$BaCo_{0.7}Fe_{0.22}Y_{0.08}O_{3-\delta}$ as an active oxygen reduction electrode for low temperature solid oxide fuel cells below 600 °C

Wei He [a], Xuelian Wu [b], Guangming Yang [c], Huangang Shi [d], Feifei Dong [a,*], Meng Ni [a,*]

[a] *Building Energy Research Group, Department of Building and Real Estate, The Hong Kong Polytechnic University, Hung Hom, Kowloon, Hong Kong 999077, China*

[b] *Department of Physics and Materials Science, City University of Hong Kong, Tat Chee Avenue, Kowloon, Hong Kong 999077, China*

[c] *State Key Laboratory of Materials-Oriented Chemical Engineering, College of Chemical Engineering, Nanjing Tech University, No. 5 Xin Mofan Road, Nanjing 210009, China*

[d] *School of Environmental Engineering, Nanjing Institute of Technology, Nanjing 211167, China*

*** Corresponding authors. Tel.: +852 2766 4152; fax: +852 2764 5131.**

E-mail addresses: ff.dong@polyu.edu.hk, meng.ni@polyu.edu.hk

Abstract

A novel B-site Y-doped perovskite $BaCo_{0.7}Fe_{0.22}Y_{0.08}O_{3-\delta}$ (BCFY) demonstrates an extremely low polarization resistance, e.g. 0.10 Ω cm^2 at 550 °C, which is ascribed to the high cubic symmetry structure and fast oxygen kinetics. The excellent electrocatalytic performance enables BCFY to be a promising cathode material towards the application of reduced temperature solid oxide fuel cells.

Keywords: Solid oxide fuel cell; Cathode; Perovskite; Y-doping; Electrochemical performance

1. Introduction

Solid oxide fuel cells (SOFCs) are sustainable energy conversion devices that can directly convert chemical energy in fuel to electrical power, with high chemical-to-electrical efficiency, flexible fuel sources, and low emissions [1-2]. Recently, extensive efforts to SOFCs have been focused on lowering operating temperature, especially below 600 °C [3-5], which allows more inexpensive interconnecting materials (stainless steel), more elegant sealing, and better thermal and chemical stability of the cell components [6]. Central to this device is the availability of a highly active oxygen reduction reaction (ORR) catalyst [7], especially at reduced temperatures.

The mixed ionic-electronic conductors (MIECs) can extend the active sites for ORR from a conventional electrode-electrolyte-air triple phase boundary (TPB) region to the entire electrode surface, thus significantly enhancing electrode activity. Among them, cobalt-containing perovskite oxides, such as $Ba_{0.5}Sr_{0.5}Co_{0.8}Fe_{0.2}O_{3-\delta}$ (BSCF), $Sm_{0.5}Sr_{0.5}CoO_{3-\delta}$ (SSC), $La_{0.6}Sr_{0.4}Co_{0.2}Fe_{0.8}O_{3-\delta}$ (LSCF), and $SrNb_{0.1}Co_{0.9}O_{3-\delta}$ (SNC), [4][8-12], have been extensively investigated as effective cathode materials for low-temperature SOFCs (LT-SOFCs).

As an important parent oxide, many perovskite-type composite oxides with a large diversity of properties can be developed based on $BaCo_{1-x}Fe_xO_3$ (BCF), which exhibits favorable oxygen-ion migration because of sufficient lattice free volume and good catalytic activity for ORR due to variable valence state of Co/Fe ions [13]. However, because of the large ionic size mismatch between Ba and Co/Fe ions, the BCF usually

prefers the low-symmetry hexagonal phase. The formation energy of an oxygen vacancy in the hexagonal phase is much higher than that in the cubic phase [14]. For stabilizing the cubic lattice structure, a doping strategy is often applied. Smaller ions such as Sr and La, were used to partially replace the large Ba ions in A site [4][15-16], or cations with both a high valence state and large size were doped into the Co/Fe site to stabilize the cubic structure of BCF, as a result, the resulting composite oxide showed very promising electrochemical activity for ORR, such as $BaCo_{0.7}Fe_{0.2}Nb_{0.1}O_{3-\delta}$ [17], $BaCo_{0.4}Fe_{0.4}Zr_{0.2}O_{3-\delta}$ [18], $BaCo_{0.7}Fe_{0.2}Ta_{0.1}O_{3-\delta}$ [19], and $BaCo_{0.7}Fe_{0.2}Sn_{0.1}O_{3-\delta}$ [15-19][20-21]. Recently, cubic perovskite-type oxides $BaCo_{0.7}Fe_{0.3-x}Y_xO_{3-\delta}$ ($BCFY_x$) have been attracted much attention as ceramic membranes for oxygen separation from air [22]. It was claimed that the Y-substitution stabilized the cubic structure because of its large size and increased the oxygen vacancy concentration for its low valence state, and the ceramic membranes showed a high oxygen permeation flux. Till now, however, detailed knowledge about the electrochemical properties of $BCFY_x$ as oxygen reduction electrocatalyst for LT-SOFCs is still unclear.

Herein, we present a B-site Y^{3+} doped perovskite-type oxide with a nominal composition of $BaCo_{0.7}Fe_{0.22}Y_{0.08}O_{3-\delta}$ (BCFY) towards the application as an oxygen reduction electrode. The cubic phase structure and fast oxygen kinetics of BCFY perovskite render it a promising cathode material with the desirable electrochemical activity for LT-SOFCs.

2. Experimental

2.1. Powder preparation

BCFY powder was synthesized by a combined EDTA-citric complexing sol-gel process. Analytic reagents of $Ba(NO_3)_2$, $Co(NO_3)_2{\cdot}6H_2O$, $Fe(NO_3)_3{\cdot}9H_2O$ and $Y(NO_3)_3{\cdot}6H_2O$ were used as metal sources. The stoichiometric amounts of above metal ions were dissolved into de-ionized water, then EDTA and citric acid were added as complexing agents at a mole ratio of 1 : 1 : 2 for total metal ions : EDTA : citric acid, and $NH_3{\cdot}H_2O$ was used to adjust the pH value of the solution to ~7. After heating with stirring, a transparent gel was attained, which was subsequently pre-fired at 250 °C to form a black solid precursor, and then calcined at 900 °C for 2 h in air to obtain the BCFY powder. For comparison on electrocatalytic activity, BSCF powder was also synthesized using the similar process.

2.2. Material characterization

The crystal structure of BCFY powder was determined by X-ray diffraction (XRD, Rigaku Smartlab) with filtered Cu Kα radiation. The experimental diffraction pattern was collected in a step-scan mode over a range of 20-80° with intervals of 0.02°. The obtained diffraction pattern was analyzed using the Rietveld method with the Fullprof software [23]. The microstructure and morphology of specimen were investigated using scanning electron microscope (SEM, JEOL 6490) and scanning transmission electron microscope (STEM, JEOL JEM-2100F) equipped with energy dispersive X-ray (EDX). The bar-shaped dense specimens were prepared by dry pressing followed by sintering for conductivity testing, which was performed using a four-probe DC method with a

Keithley 2420 source meter. For the electrical conductivity measurement, it was conducted over a temperature range of 400-700 °C. For the electrical conductivity relaxation (ECR) measurement, used to characterize the oxygen kinetics over the cathode materials, e.g., surface exchange and bulk diffusion, the oxygen partial pressure of N_2-O_2 mixture was abruptly changed from 0.21 to 0.1 atm. The variation of conductivity was recorded continuously as a function of relaxation time until it finally got equilibrium.

2.3. Symmetrical cell and single cell fabrication

Symmetrical cells with a BCFY|SDC|BCFY configuration were fabricated for electrochemical impedance studies. Dense SDC substrates were prepared through dry pressing with subsequent calcination at 1350 °C for 5 h. BCFY powder was dispersed with glycol, ethylene glycol, and isopropyl alcohol to form a colloidal suspension through ball milling. The resulting electrode slurries were sprayed symmetrically onto both surfaces of the SDC disks and subsequently fired at 900 °C for 0.5 h in air to form the symmetrical cells. Silver paste was then applied onto the electrode surface as the current collector. As a reference, the BSCF|SDC|BSCF symmetrical cells were prepared and measured under the identical conditions. The anode-supported dual-layer cells were fabricated using a dry-press and co-sintering technique. The well-mixed NiO + SDC (weight ratio 3:2) anode powders by ball milling were first pressed as a substrate, onto which the fine SDC powders were added and pressed again to form bilayer pellets. The green pellets were then sintered in air at 1350 °C for 5 h for the densification of

electrolyte layer. Subsequently, BCFY slurries were spray-deposited on the central surface of the electrolyte. The completed triple-layered cells were finally fired at 900 °C for 0.5 h in air.

2.4. Electrochemical evaluation and fuel cell testing

The electrode polarization resistance was measured using an electrochemical workstation based on a Solartron 1260A frequency response analyzer in combination with a Solartron 1287 potentiostat. The frequency applied of electrochemical impedance spectroscopy (EIS) was ranged from 0.01 Hz to 1 MHz with a signal amplitude of 10 mV. The electrochemical performance of single cells was tested over a home-made fuel cell testing station. Humidified hydrogen fuel was fed into the anode chamber at a flow rate of 100 mL min^{-1}, and ambient air served as the oxidant gas in the cathode chamber. I-V polarization curves were collected using a Keithley 2420 digital source meter based on the four-probe configuration at 450-600 °C.

3. Results and discussion

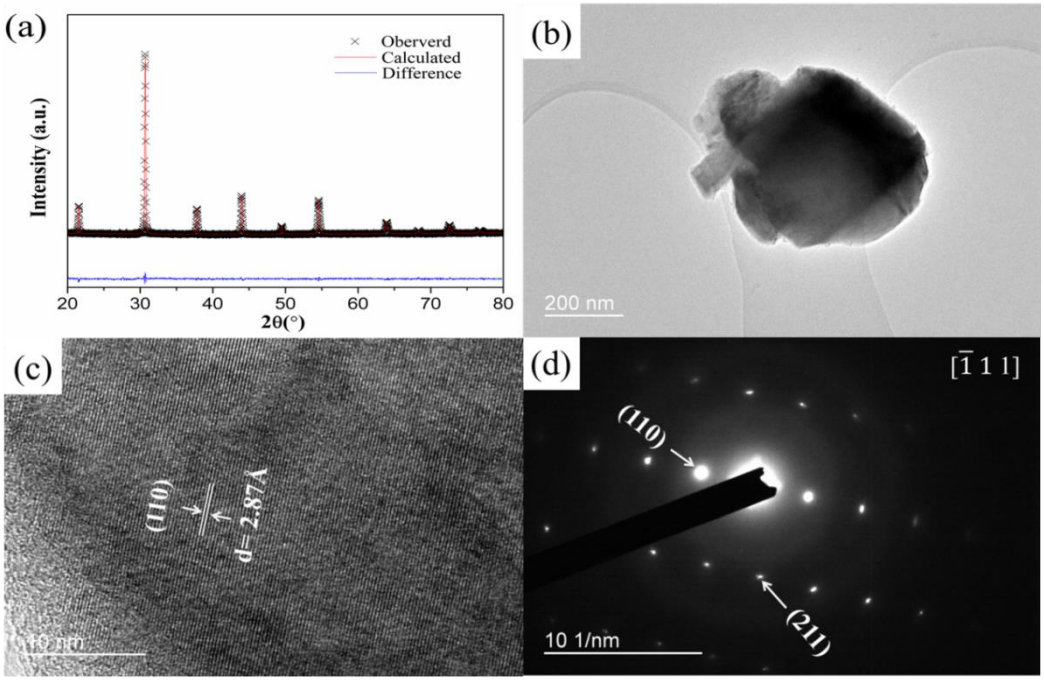

Fig. 1. (a) XRD pattern of BCFY powder, (b) TEM image of BCFY, (c) a high-resolution TEM image, (d) the corresponding SEAD patterns

Fig. S1 exhibits the XRD patterns of the as-synthesized $BaCo_{0.7}Fe_{0.3}O_{3-\delta}$ (BCF) and BCFY oxides. The diffraction peaks of BCF oxide cannot be well indexed into a single perovskite phase, and the BCF sample consists of a major hexagonal phase and a trace amount of impurity phase. After substituting Y^{3+} cations for Fe-site, the single perovskite phase is successfully formed, suggesting that Y doping can effectively stabilize the phase structure of BCF. Fig. 1a shows the refined diffraction patterns of the as-prepared BCFY powder. It is clear that the diffraction patterns can be assigned to a cubic symmetrical perovskite structure in space group Pm-3m with unit cell data of a = 4.12 Å. The low converged reliability factors (R_p = 2.58 %, R_{wp} = 3.26 %, χ^2 = 1.32) indicate a good fitting between the experimental and calculated patterns. STEM was employed to further check the morphology and structure of BCFY. Fig. 1b is a

typical TEM image of BCFY grain synthesized by a sol-gel method. The high-resolution TEM image (Fig. 1c) exhibits the presence of crystalline fringes, corresponding to the (110) crystal plane of the cubic perovskite structure, with a lattice fringe spacing of d_{110} = 2.87 Å. The crystal structure is also confirmed to be perovskite from the corresponding selected area electron diffraction (SAED) patterns (Fig. 1d) along the $[\bar{1}11]$ zone axis. The result above is in accordance with the XRD data (d_{110} = 2.89 Å). The existence of Ba, Co, Fe, and Y can be validated by the EDX diffraction spectrum (Fig. S2). As reported before, BCF has a hexagonal perovskite structure and its Goldschmidt tolerance factor $t = (r_A + r_O)/\sqrt{2}\ (r_B + r_O)$ is estimated to be bigger than 1. The partial substitution of Y ions with a larger ionic radius ($r_{Y^{3+}}$ = 0.90 Å) for B-site Fe ions ($r_{Fe^{3+}}$ = 0.645 Å, $r_{Fe^{4+}}$ = 0.585 Å) enables it to approach to 1, which contributes to the construction of cubic perovskite structure [24].

The dependences of electrical conductivity of BCFY on temperature (400-700 °C) and oxygen partial pressure (PO_2 = 0.21 and 0.1 atm) are shown in Fig. S3. The electrical conductivity increases monotonously with an increase in temperature, suggesting a semi-conducting behavior. Identification of oxygen bulk diffusion coefficient (D_{chem}) and surface exchange coefficient (k_{chem}), measured using ECR technique, can be helpful in evaluating the electrocatalytic activity of electrode materials. Fig. 2a depicts the typical transient conductivity response of BCFY within the temperature range of 450-750 °C upon abruptly shifting the oxygen partial pressure from 0.21 to 0.1 atm. The Arrhenius plots of D_{chem} and k_{chem} for BCFY perovskite are shown in Fig. 2b, both D_{chem} and k_{chem} values rise with an increase in temperature, indicating high activity at elevated

temperatures. Lower activation energies for D_{chem} and k_{chem} indicate that the oxygen kinetics has low temperature dependence, in favor of reduced temperature operation. The high D_{chem} and k_{chem} values of 2.24×10^{-4} cm^2 s^{-1} and 2.23×10^{-3} cm s^{-1} at 600 °C are obtained, which are much larger than those of other prevalent cathode materials, such as LSCF [25] and BSCF [26]. Additionally, the electrical conductivity of BCFY is smaller than that of LSCF [27] and BSCF [28], implying that the improved activity is not attributed to the electronic conductivity.

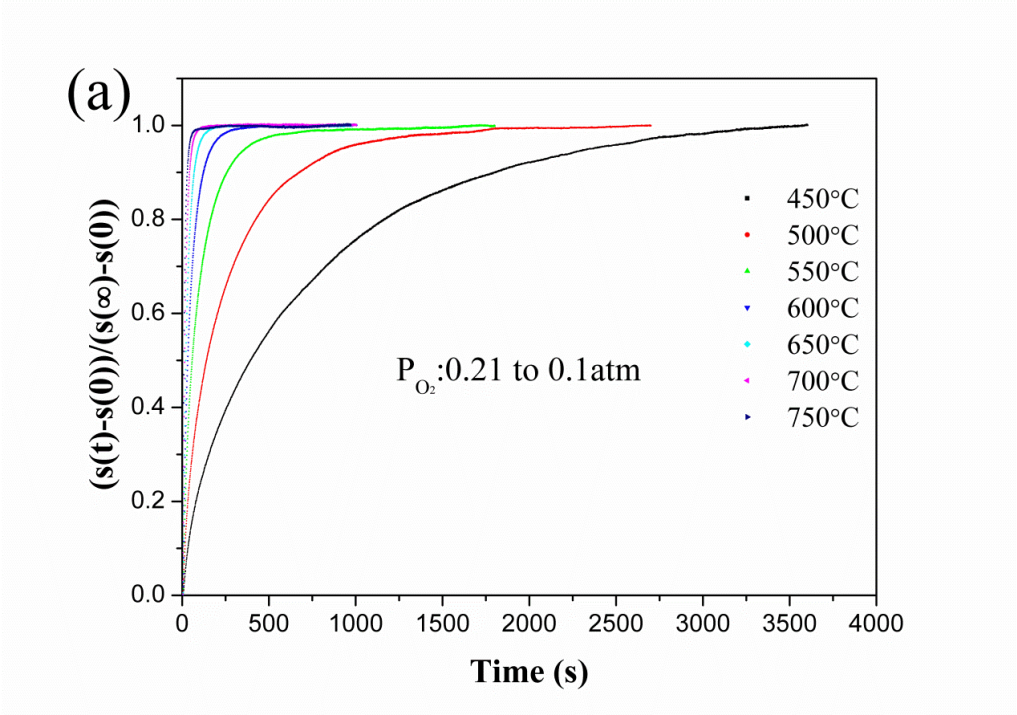

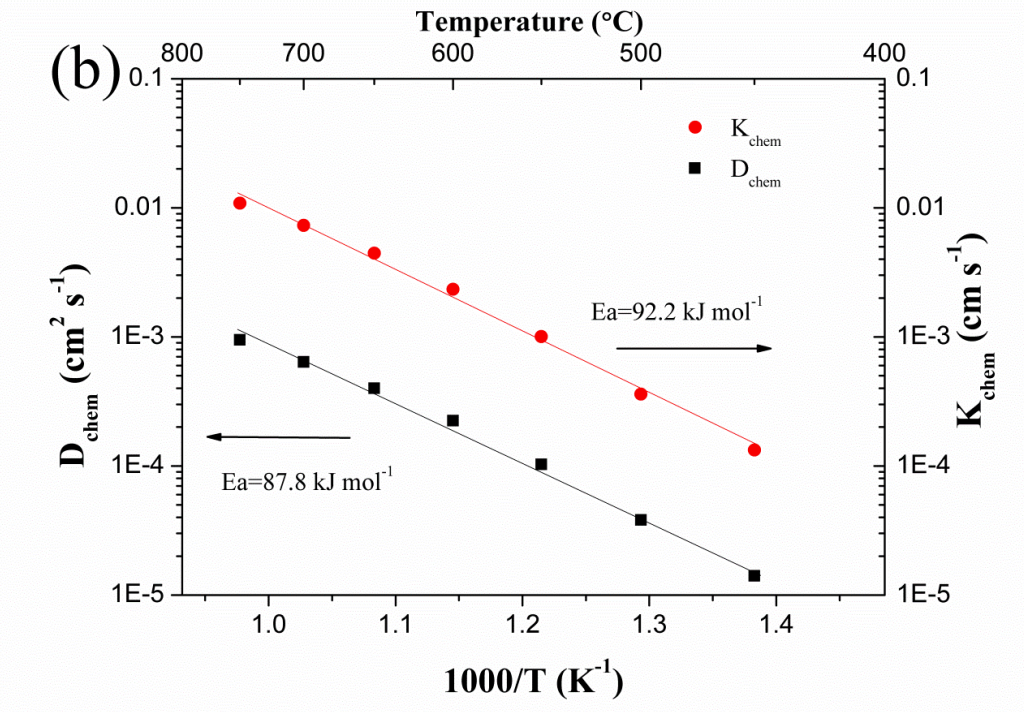

Fig. 2. (a) ECR responses of BCFY at various temperatures after an abrupt change of oxygen partial pressure from 0.21 to 0.1 atm, (b) Variation of D_{chem} and k_{chem} for BCFY with respect to temperature derived from the ECR measurement

The area specific resistance (ASR) of BCFY was measured by EIS for BCFY|SDC|BCFY symmetrical cell configuration. The ASR values are determined by the impedance intercept between high-frequency and low-frequency on the real axis of the Nyquist plot, and representative impedance spectra are presented in Fig. S4a. The ASR values are 0.03, 0.10, and 0.43 Ω cm^2 at 600, 550, and 500 °C respectively. The extremely low electrode polarization resistance reflects high activity for ORR. For comparison, the ASRs of a benchmark cathode-BSCF are measured to be 0.09, 0.23, and 1.1 Ω cm^2 at 600, 550, and 500 °C, respectively (Fig. S4b), approximately 1-2 times higher than those of BCFY cathode. As shown in Fig. 3, the BCFY cathode exhibits

lower ASRs than those of the predominant cobalt-containing cathode materials, such as LSCF and SSC [9,11]. Additionally, the ASR values of BCFY cathode are much lower than those of other BCF-derived cathode materials like $BaCo_{0.7}Fe_{0.2}Nb_{0.1}O_{3-\delta}$ and $BaCo_{0.7}Fe_{0.2}Sn_{0.1}O_{3-\delta}$ [17]. It thus suggests the superior electrocatalytic activity of BCFY for ORR, which relates well with high cubic symmetry structure and fast oxygen bulk diffusion and surface exchange kinetics.

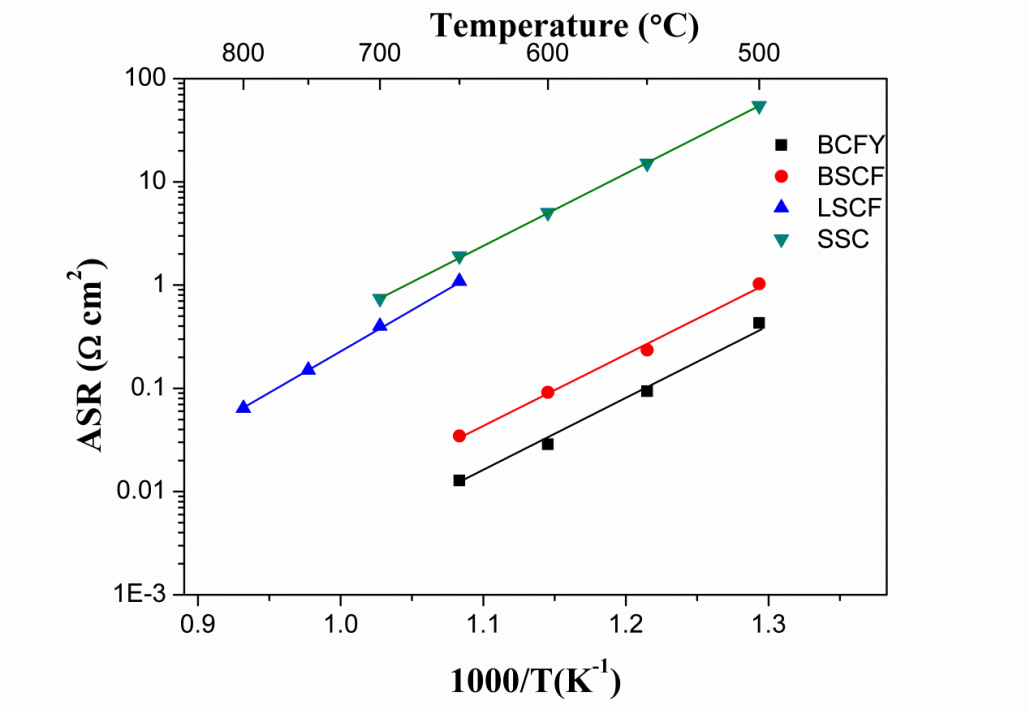

Fig. 3. Arrhenius-type plots of ASR values for BCFY cathode and other predominant cobalt-containing perovskite cathodes at various temperatures

The electrochemical performance of BCFY cathode for ORR was further tested in a single cell configuration under real fuel cell operation conditions. Fig. S5 exhibits a typical SEM image of the anode-supported triple-layered fuel cell. The dense electrolyte film is ~10 μm-thick and is well-adhered to the electrodes, without any

noticeable cracking or delamination. Fig. 4 shows the I-V polarization curves and the corresponding power density curves obtained for the single cell using humidified H_2 (3% H_2O) as a fuel and static ambient air as an oxidant over a temperature range of 450-600 °C. The cell exhibits superior open circuit voltages (OCVs) from 0.86 V (600 °C) to 0.94 V (500 °C), which are lower than the theoretical values because of some internal short-circuits in SDC electrolyte caused by partial reduction of Ce^{4+} ions to Ce^{3+} ions [29]. The cell delivers an attractive power output with peak power densities of 967, 687, and 423 mW cm^{-2} at 600, 550, and 500 °C, respectively, which are comparable to those of BSCF under similar operation conditions [4]. The fuel cell performance can be affected by many resistances, such as contact resistance between electrode and current collector, electrode polarization resistance, concentration polarization resistance, electrolyte resistance and so on. The fuel cells with BCFY cathode do not show a higher performance although the cathode exhibits a lower ASR value than that of BSCF, it might relate to other resistances. As shown in Fig. S6, under a constant current density of 400 mA cm^{-2}, a stable voltage at around 0.75 V is achieved throughout a test period of 50 h at 550 °C. The favorable cell performance and stability test suggest the BCFY holds a great promise as an oxygen reduction electrode for application in LT-SOFC field.

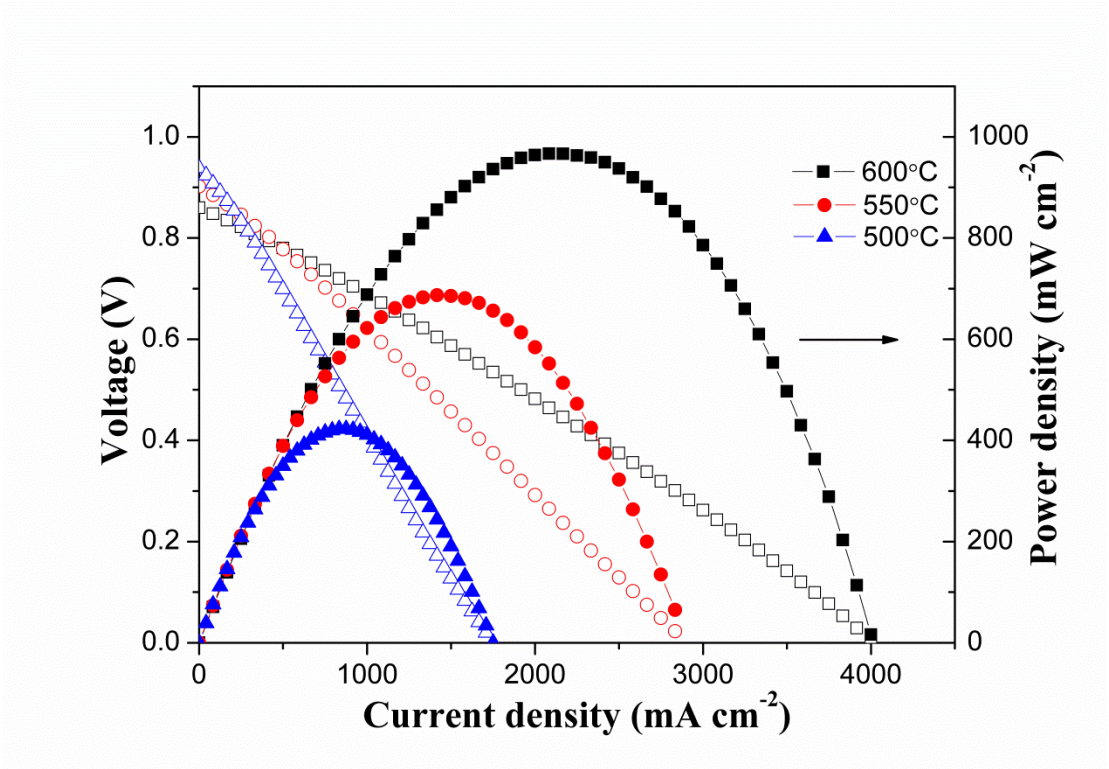

Fig. 4. I-V curves and corresponding power densities of single cell at different temperatures

4. Conclusions

A cubic symmetry perovskite oxide BCFY was achieved by substituting 8% mol Y for Fe in B-site, and its properties were characterized. The obtained extremely low polarization resistance values can be attributed to the cubic symmetrical structure and fast oxygen bulk diffusion and surface exchange properties. The favorable electrochemical activity and stability justify the potential of BCFY as an active oxygen reduction electrode for reduced temperature SOFCs.

Acknowledgements

This study was supported by a grant (Project Number: PolyU 152127/14E) from Research Grant Council, University Grants Committee, Hong Kong SAR, a grant from The Hong Kong Polytechnic University (Account: 1-ZVFQ), and National Natural Science Foundation of China (Contract No. 51302135).

Appendix A. Supplementary data

Supplementary data related to this article can be found at

References

1. Singhal, S. C., Advances in solid oxide fuel cell technology. *Solid State Ionics* **2000,** *135* (1-4), 305-313.
2. Jacobson, A. J., Materials for Solid Oxide Fuel Cells. *Chem Mater* **2010,** *22* (3), 660-674.
3. Wachsman, E. D.; Lee, K. T., Lowering the Temperature of Solid Oxide Fuel Cells. *Science* **2011,** *334* (6058), 935-939.
4. Shao, Z. P.; Haile, S. M., A high-performance cathode for the next generation of solid-oxide fuel cells. *Nature* **2004,** *431* (7005), 170-173.
5. Wachsman, E. D.; Marlowe, C. A.; Lee, K. T., Role of solid oxide fuel cells in a balanced energy strategy. *Energ Environ Sci* **2012,** *5* (2), 5498-5509.
6. Fergus, J. W., Metallic interconnects for solid oxide fuel cells. *Mat Sci Eng a-Struct* **2005,** *397* (1-2), 271-283.
7. Steele, B. C. H.; Heinzel, A., Materials for fuel-cell technologies. *Nature* **2001,** *414* (6861), 345-352.
8. Xia, C. R.; Rauch, W.; Chen, F. L.; Liu, M. L., Sm0.5Sr0.5CoO3 cathodes for low-temperature SOFCs. *Solid State Ionics* **2002,** *149* (1-2), 11-19.
9. Dong, F. F.; Chen, D. J.; Ran, R.; Park, H.; Kwak, C.; Shao, Z. P., A comparative study of Sm0.5Sr0.5MO3-delta (M = Co and Mn) as oxygen reduction electrodes for solid oxide fuel cells. *Int J Hydrogen Energ* **2012,** *37* (5), 4377-4387.
10. Leng, Y. J.; Chan, S. H.; Liu, Q. L., Development of LSCF-GDC composite cathodes for low-temperature solid oxide fuel cells with thin film GDC electrolyte. *Int J Hydrogen Energ* **2008,** *33* (14), 3808-3817.
11. Nie, L. F.; Liu, M. F.; Zhang, Y. J.; Liu, M. L., La0.6Sr0.4Co0.2Fe0.8O3-delta cathodes infiltrated with samarium-doped cerium oxide for solid oxide fuel cells. *J Power Sources* **2010,** *195* (15), 4704-4708.
12. Zhou, W.; Shao, Z. P.; Ran, R.; Jin, W. Q.; Xu, N. P., A novel efficient oxide electrode for

electrocatalytic oxygen reduction at 400-600 degrees C. *Chem Commun* **2008,** (44), 5791-5793.

13. Sammells, A. F.; Cook, R. L.; White, J. H.; Osborne, J. J.; Macduff, R. C., Rational Selection of Advanced Solid Electrolytes for Intermediate Temperature Fuel-Cells. *Solid State Ionics* **1992,** *52* (1-3), 111-123.

14. Yoshiya, M.; Fisher, C. A. J.; Iwamoto, Y.; Asanuma, M.; Ishii, J.; Yabuta, K., Phase stability of BaCo1-yFeyO3-delta by first principles calculations. *Solid State Ionics* **2004,** *172* (1-4), 159-163.

15. Zhou, W.; Ran, R.; Shao, Z. P., Progress in understanding and development of Ba0.5Sr0.5Co0.8Fe0.2O3-delta-based cathodes for intermediate-temperature solid-oxide fuel cells: A review. *J Power Sources* **2009,** *192* (2), 231-246.

16. Kim, J.; Choi, S.; Jun, A.; Jeong, H. Y.; Shin, J.; Kim, G., Chemically Stable Perovskites as Cathode Materials for Solid Oxide Fuel Cells: La-Doped Ba0.5Sr0.5Co0.8Fe0.2O3-delta. *Chemsuschem* **2014,** *7* (6), 1669-1675.

17. Harada, M.; Domen, K.; Hara, M.; Tatsumi, T., Oxygen-permeable membranes of Ba1.0Co0.7Fe0.2Nb0.1O3-delta for preparation of synthesis gas from methane by partial oxidation. *Chem Lett* **2006,** *35* (8), 968-969.

18. Shang, M.; Tong, J. H.; O'Hayre, R., A promising cathode for intermediate temperature protonic ceramic fuel cells: BaCo(0.4)Fe(0.4)Zr(0.2)O3-delta. *Rsc Adv* **2013,** *3* (36), 15769-15775.

19. Xie, K.; Zhou, J. E.; Meng, G. Y., Pervoskite-type BaCo0.7Fe0.2Ta0.1O3-delta cathode for proton conducting IT-SOFC. *J Alloy Compd* **2010,** *506* (1), L8-L11.

20. Qian, B. M.; Chen, Y. B.; Tade, M. O.; Shao, Z. P., BaCo0.6Fe0.3Sn0.1O3-delta perovskite as a new superior oxygen reduction electrode for intermediate-to-low temperature solid oxide fuel cells. *J Mater Chem A* **2014,** *2* (36), 15078-15086.

21. Zhang, Z. B.; Chen, Y. B.; Tade, M. O.; Hao, Y.; Liu, S. M.; Shao, Z. P., Tin-doped perovskite mixed conducting membrane for efficient air separation. *J Mater Chem A* **2014,** *2* (25), 9666-9674.

22. Zhao, H. L.; Xu, N. S.; Cheng, Y. F.; Wei, W. J.; Chen, N.; Ding, W. Z.; Lu, X. G.; Li, F. S., Investigation of Mixed Conductor BaCo0.7Fe0.3-xYxO3-delta with High Oxygen Permeability. *J Phys Chem C* **2010,** *114* (41), 17975-17981.

23. Rodríguez-Carvajal, J., Recent developments of the program FULLPROF. *Commission on powder diffraction (IUCr). Newsletter* **2001,** *26*, 12-19.

24. Shao, Z. P.; Xiong, G. X.; Tong, J. H.; Dong, H.; Yang, W. S., Ba effect in doped Sr(Co0.8Fe0.2)O3-delta on the phase structure and oxygen permeation properties of the dense ceramic membranes. *Sep Purif Technol* **2001,** *25* (1-3), 419-429.

25. Pakzad, A.; Salamati, H.; Kameli, P.; Talaei, Z., Preparation and investigation of electrical and electrochemical properties of lanthanum-based cathode for solid oxide fuel cell. *Int J Hydrogen Energ* **2010,** *35* (17), 9398-9400.

26. Chen, D. J.; Shao, Z. P., Surface exchange and bulk diffusion properties of Ba0.5Sr0.5Co0.8Fe0.2O3-delta mixed conductor. *Int J Hydrogen Energ* **2011,** *36* (11), 6948-6956.

27. Xu, S. J.; Thomson, W. J., Oxygen permeation rates through ion-conducting perovskite membranes. *Chem Eng Sci* **1999,** *54* (17), 3839-3850.

28. Wei, B.; Lu, Z.; Huang, X. Q.; Miao, J. P.; Sha, X. Q.; Xin, X. S.; Su, W. H., Crystal structure, thermal expansion and electrical conductivity of perovskite oxides BaxSr1-xCo0.8Fe0.2O3-delta (0.3 <= x <= 0.7). *J Eur Ceram Soc* **2006,** *26* (13), 2827-2832.

29. Zhang, X.; Robertson, M.; Deces-Petit, C.; Qu, W.; Kesler, O.; Maric, R.; Ghosh, D., Internal shorting and fuel loss of a low temperature solid oxide fuel cell with SDC electrolyte. *J Power Sources* **2007,** *164*

(2), 668-677.

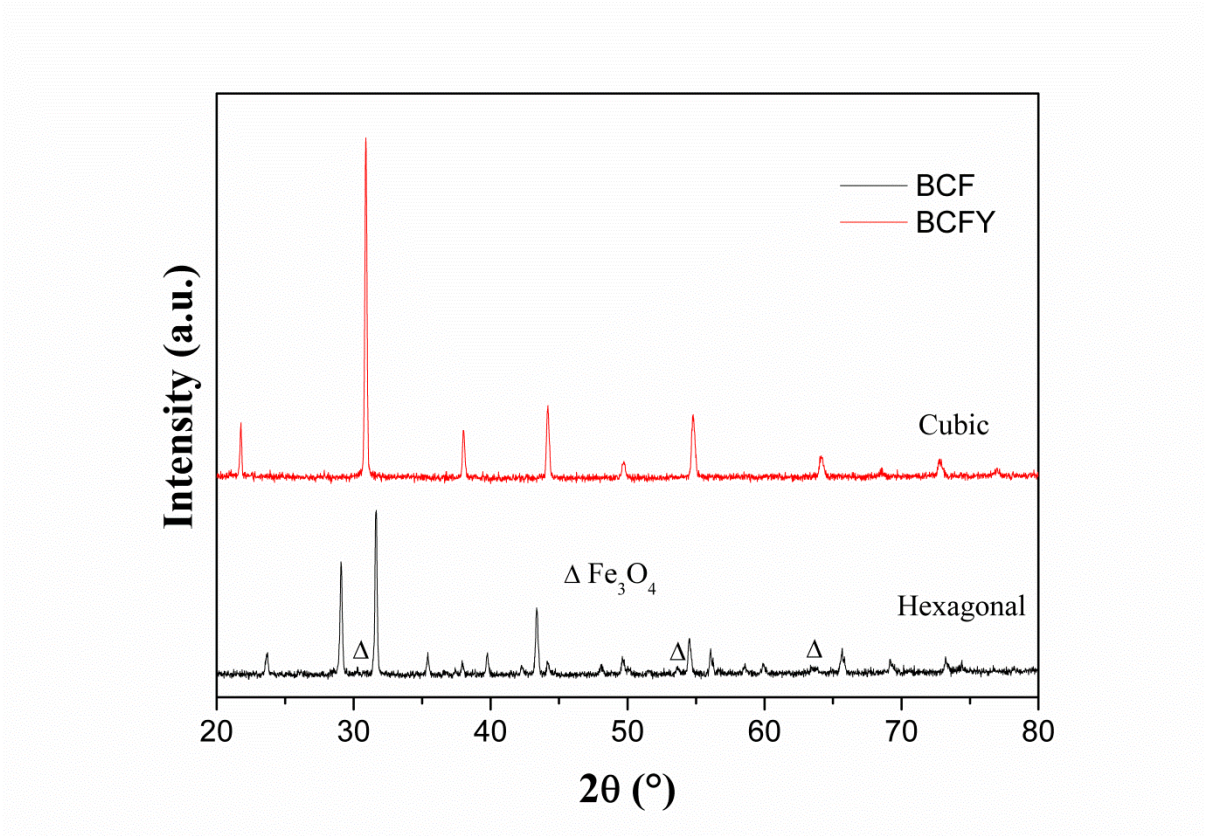

Fig. S1 XRD patterns of BCF and BCFY

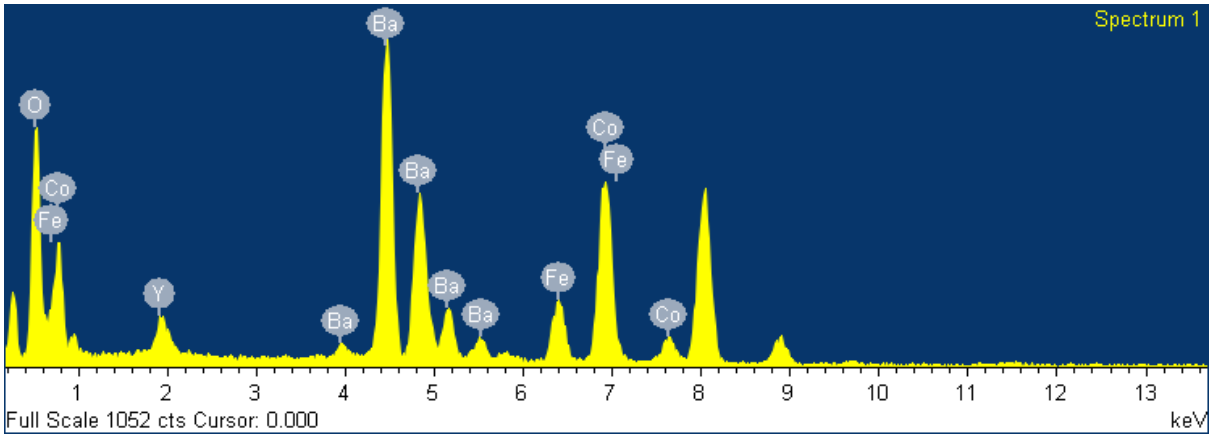

Fig. S2 EDX diffraction spectrum of BCFY powder

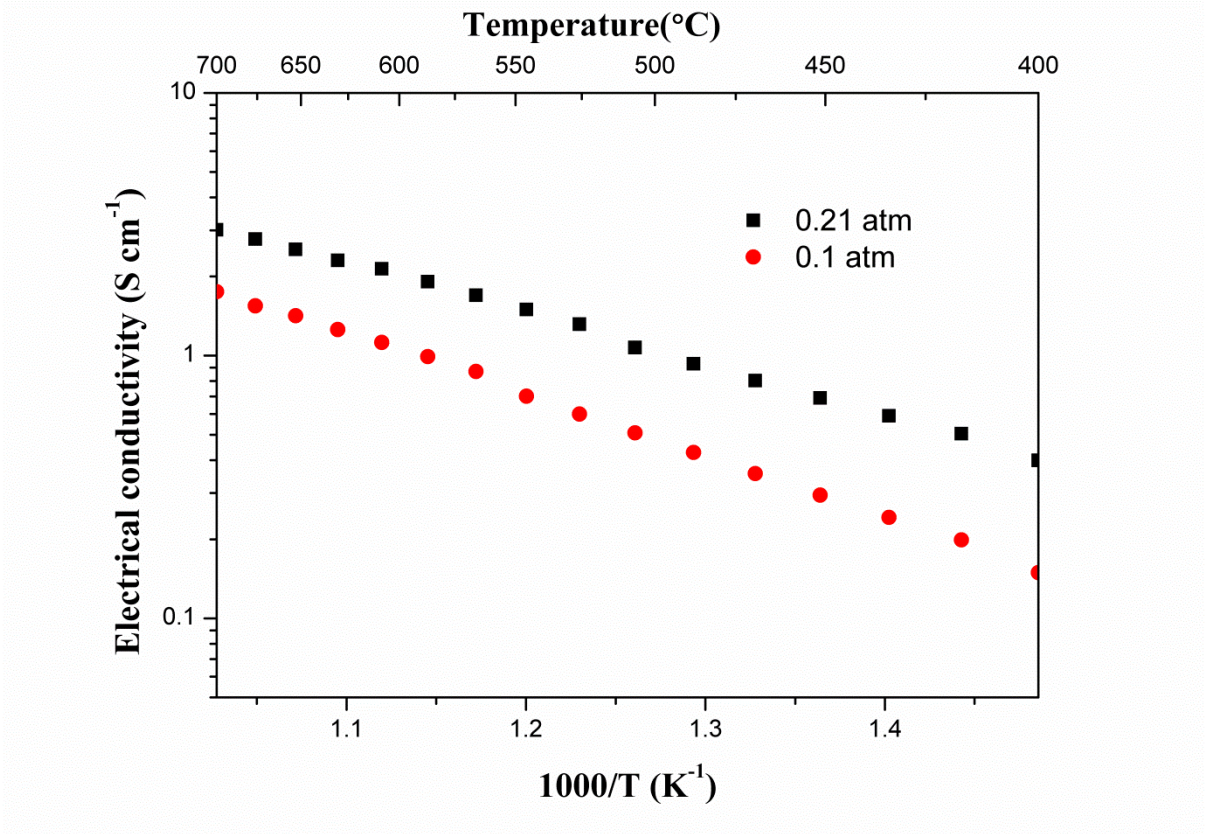

Fig. S3 Electrical conductivity of BCFY in 21% and 10% oxygen pressure as a function of
Temperature

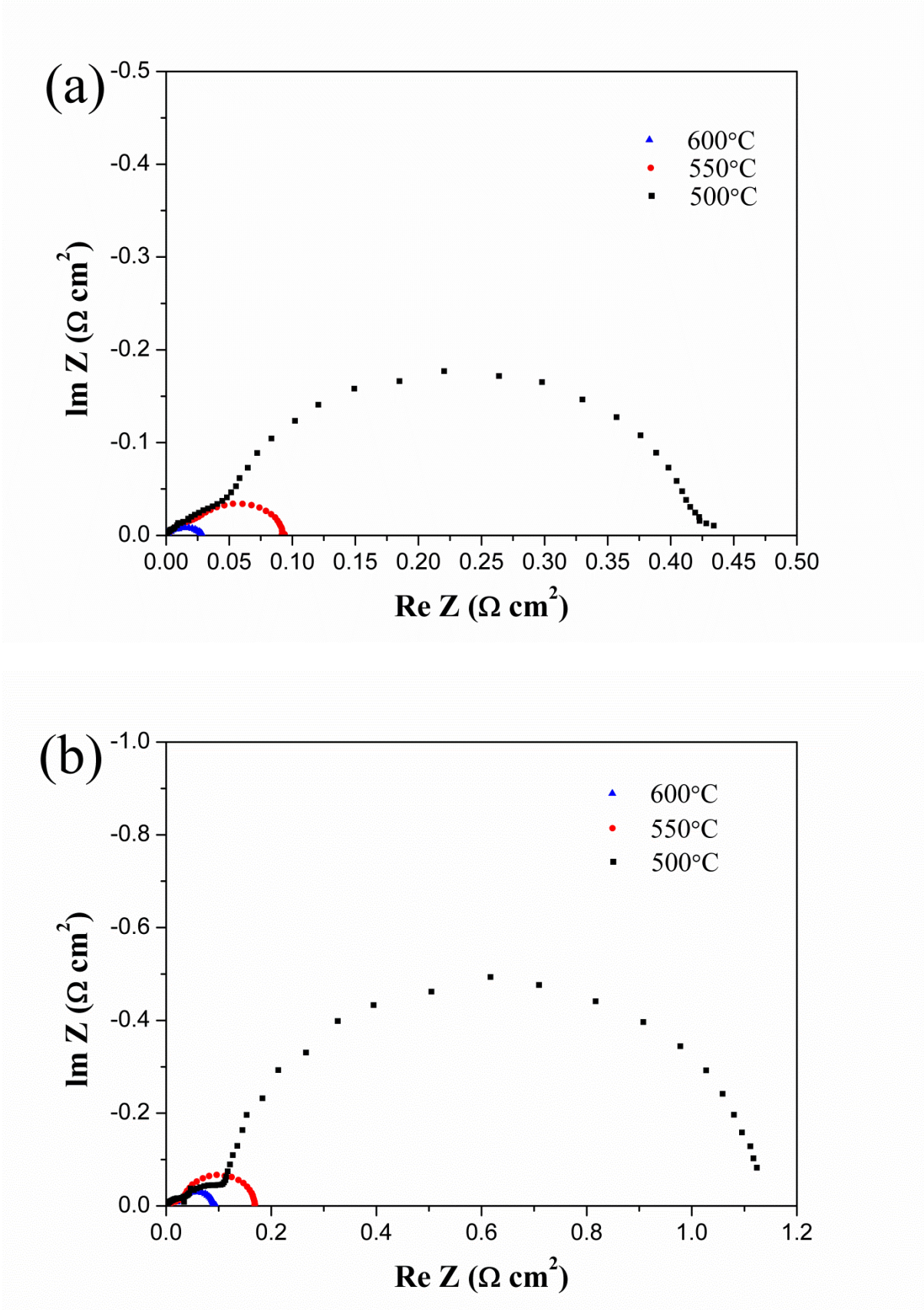

Fig. S4 Impedance spectra of cathodes at 500 550 and 600ºC (a) BCFY cathode (b) BSCF cathode

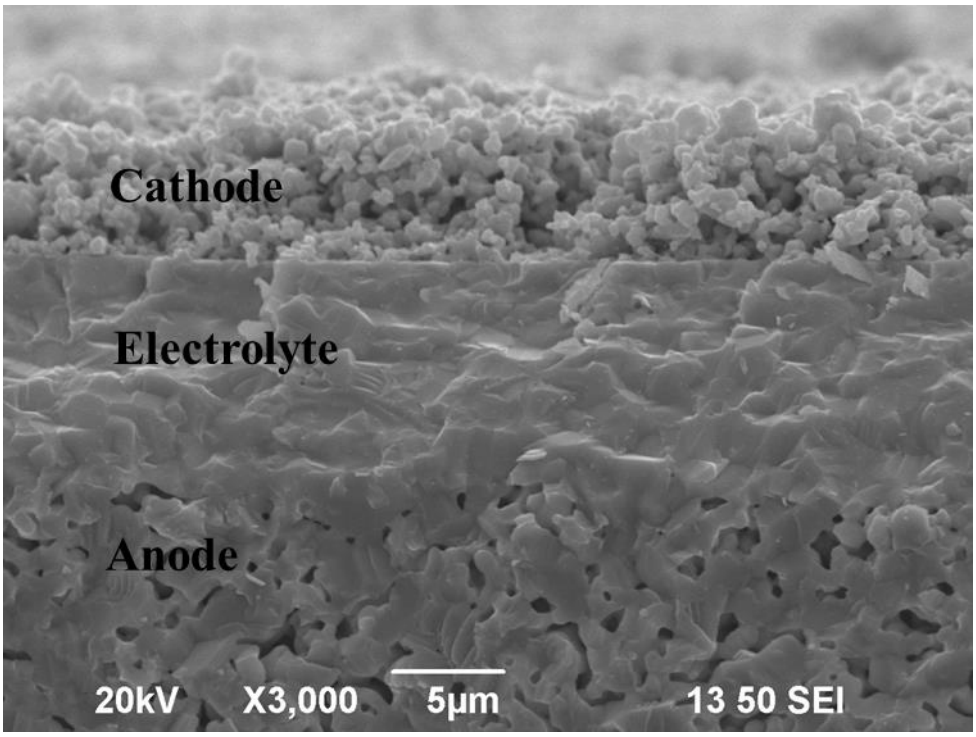

Fig. S5 Cross section of a button fuel cell along the thickness direction

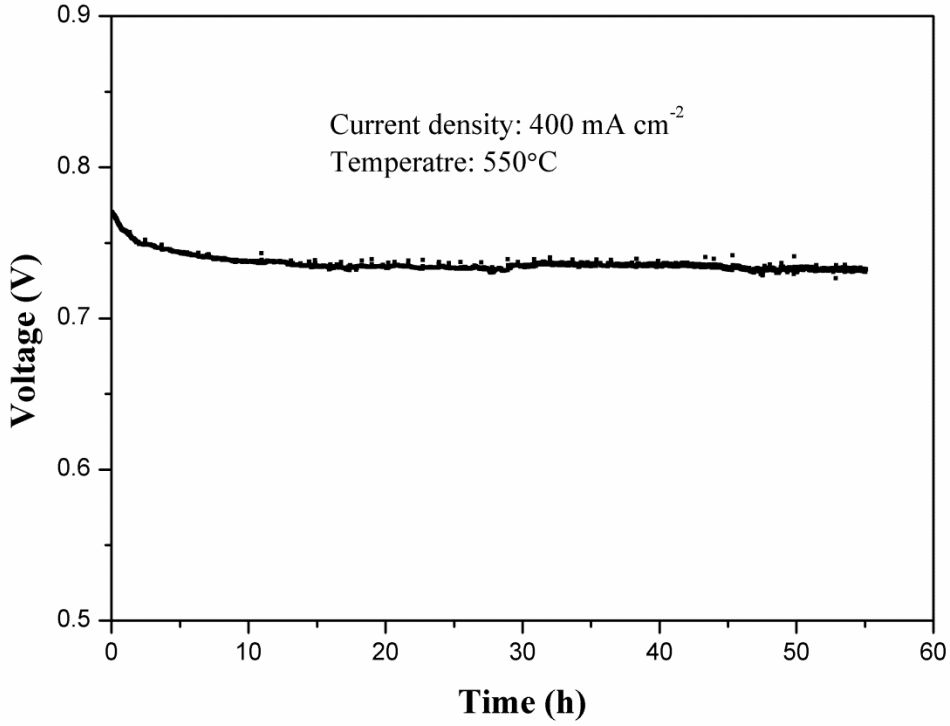

Fig. S6 The stability test of a single cell with a BCFY cathode at 550°C